

Brain Activity Measurement during a Mental Arithmetic Task in fNIRS Signal Using Continuous Wavelet Transform

Farzaneh Aliabadi Farahani ¹, Mehrdad Dadgostar ^{1,*} , Zahra Einalou ²

¹ Department of Biomedical Engineering, Central Tehran Branch, Islamic Azad University, Tehran, Iran

² Department of Biomedical Engineering, North Tehran Branch, Islamic Azad University, Tehran, Iran

*Corresponding Author: Mehrdad Dadgostar
Email: m.dadgostar@iauctb.ac.ir

Received: 25 April 2021 / Accepted: 17 July 2021

Abstract

Purpose: Functional Near-Infrared Spectroscopy (fNIRS) is a non-invasive imaging technology with widespread use in cognitive sciences and clinical studies. It indirectly measures neural activation by measuring alterations of oxyhemoglobin (HbO₂) and deoxyhemoglobin (Hb) in tissues. This study used mental arithmetic task for analyzing the activation of the frontal cortex.

Materials and methods: The fNIRS instrument was used for measuring the alterations of HbO₂ and Hb in healthy subjects during the task. Then the recorded signals were filtered in the frequency range of 3 to 80 mHz. The Continuous Wavelet Transform (CWT) of each of the HbO₂ and Hb signals in each channel was calculated in the intended frequency range, followed by the calculation of the energy of obtained coefficients. Finally, for the performed tasks, the average energy of each channel in each region was obtained. Then the energies of spatially symmetric channel pairs in the two hemispheres were compared using the t-test.

Results: Results demonstrated that the average energy of HbO₂ signal for corresponding channels in the temporal, Medial Prefrontal Cortex (MPFC), and Dorsolateral Prefrontal Cortex (DLPFC) regions had significant differences ($P < 0.05$). Also, a significant difference was observed in the temporal, medial prefrontal, and Ventrolateral Prefrontal Cortex (VLPFC) regions for Hb signal.

Conclusion: The obtained results indicate activation in both HbO₂ and Hb signals in the DLPFC, temporal, and MPFC regions, considering the performance of memory and the frontal cortex under mental arithmetic tasks. Therefore, it can be concluded that this technique is effective and appropriate for analyzing alterations of brain oxygen levels during cognitive activity.

Keywords: Functional Near-Infrared Spectroscopy; Mental Arithmetic Task; Prefrontal Cortex; Continuous Wavelet Transform.

1. Introduction

Nowadays, many imaging techniques exist to measure human brain activation, including Electroencephalogram (EEG), Positron Emission Tomography (PET), functional Magnetic Resonance Imaging (fMRI) [1], and Functional Near-Infrared Spectroscopy (fNIRS). fNIRS, as an optic tool based on the neurovascular coupling theory, was first proposed more than 30 years ago in 1977 by Jobsis [2-4]. In this method, a few optodes are placed on the subject's forehead to send and receive infrared light, which passes through the skull with a specific wavelength and gets absorbed separately by the oxyhemoglobin (HbO₂) and deoxyhemoglobin (Hb) in the blood. Then, changes in the concentration are calculated using the modified Beer-Lambert law [5-8].

This method indirectly measures the neural activity of neurons [9-11]. The activity of these neurons increases the consumption of oxygen for producing energy, decreases HbO₂, and increases Hb concentration. Then, in the activated brain region, regional blood flow carrying oxygen witnesses a rise, due to oxygen shortage, which causes an increase in HbO₂ and a decrease in Hb concentration in that region [10, 12]. Readers are referred to [12-15] for further explanations on fNIRS.

Compared to other conventional neurological methods, fNIRS is known as an excellent noninvasive tool for studying brain activation, considering its acceptable spatial and temporal resolution, safety, low sensitivity to electromagnetic fields, low cost, and low-amplitude motion artifacts [12, 16-19]. This technique, however, still has downsides such as low penetration depth because of cortical layers, changing the blood flow in the scalp, and systemic changes such as increasing heart rate [12].

The current study analyzes the activity of the Prefrontal Cortex (PFC) using hemodynamic signals resulted from fNIRS of subjects under mental arithmetic tasks. Previous studies have investigated brain activation while doing this task using alterations of hemodynamic concentration by placing two-channel Near-Infrared Spectroscopy (NIRS) [20] and 16-channel NIRS [21] on the PFC of subjects. The results of the study [20] indicate the importance of the PFC in performance skills such as calculation and thinking. In research [22], different types of tasks are classified into mental arithmetic, word generation, and mental rotation categories. Then the effect of each category on the hemodynamic response of the prefrontal cortex

is examined. Using various tasks for identifying brain activation, different patterns of hemodynamic responses and brain activation are expected in different regions of the PFC [23-25]. Also, Verner *et al.* analyzed the alteration in the blood oxygen consumption using 52-channel fNIRS under a mental arithmetic task [26].

An important aspect of this study is using a simple processing algorithm for analyzing the PFC activation applying a time-frequency analysis method based on Continuous Wavelet Transform (CWT). Then, significant difference analysis between the symmetric channel pairs on the left and right hemispheres is conducted using the t-test.

The Complex Wavelet Transform method is used to reduce the physiological noise of fNIRS signal generated by heartbeat, respiration, blood pressure, and skin blood flow [27]. By using Wavelet Transform Coherence (WTC) [28], first, the temporal-frequency global noise was detected and then the signal was decomposed based on the wavelet transform, and noise was removed. Finally, the signal was reconstructed again. In our study method, in the first stage, Discrete Wavelet Transform (DWT) was used to reduce physiological noise in the frequency range of 0.003 to 0.08 Hz. In the next stage, by applying CWT and calculating the average coefficients in the time frame of 12 seconds, the hemodynamic brain activity was obtained. DWT is used to filter fNIRS signals in the frequency range of 3 to 80 mHz to better analyze the PFC activation. This method has demonstrated desirable results for removing physiological interferences in fNIRS signals and enhancing Signal to Noise Ratio (SNR) in [16, 18, 29-32]. Since fNIRS can be considered as an excellent tool to understand neural correlations with cognitive activities, the main goal of this study is to examine brain activation in the PFC region under mental arithmetic tasks using CWT analysis.

2. Materials and Methods

2.1. Subjects and Protocol

In this study, eight healthy subjects (three men and five women with an average age of 26 years, standard deviation of 2.8 years, all right-handed) participated, all of whom were without any nervous disorders, cardiovascular disease, and alcohol or drug use [33, 34] because these factors can affect the HbO₂ and Hb signals measurements.

Subjects were asked to subtract several one-digit numbers from two-digit numbers. Numbers were shown to them in 12 seconds with a frequency of once every two seconds. The experiment included three or four runs, with each run, including six blocks of task and six blocks of rest. The time required for doing the task in each block was 12 seconds, and the time for each rest was set to 28 seconds. Each subject performed 18 or 24 tasks overall. Figure 1 shows an example of the experiment protocol in a single run.

2.2. Data Acquisition

In this study, a continuous-wave NIRS (ETG4000 Hitachi japan) system was used for measuring brain activation under mental arithmetic tasks, and data were recorded from the PFC using 16 detectors and 17 light sources. In Figure 2, detectors are shown in blue and light sources in red. Channels are defined as a region

between the source and the closest detectors. The distance between each source and detector is equal to 3 cm, which has led to acceptable accordance between SNR and depth sensitivity [35]. A set of probes, including 52 channels for recording Hb and HbO₂ signals, was placed on the forehead according to the international system of 10-20 [26]. Both ends of the set of probes are symmetrically placed on T3 and T4, and the lowest row of channels is placed on the frontal position centered on Fpz and parallel with Fp1, Fp2, T3, and T4 anatomical lines from left to right [33]. The channels represent one region of the brain structure and measure the location of fNIRS signals of the Pathway Signal Flow Calculator (PSFC), Dorsolateral Prefrontal Cortex (DLPFC), temporal cortex, Ventrolateral Prefrontal Cortex (VLPFC) of the right and left hemisphere, and Medial Prefrontal Cortex (MPFC). The channel number for each region is presented in Table 1. In recording the signal, the sampling rate was set to 10 Hz.

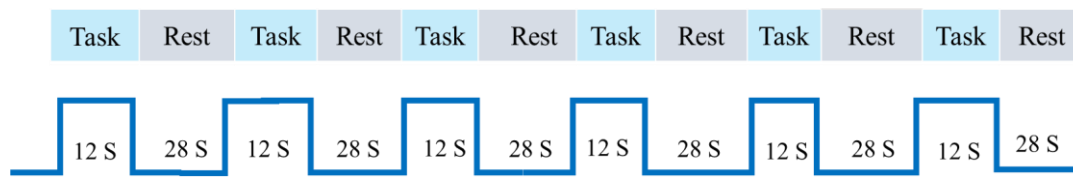


Figure 1. The mental arithmetic task structure. A single run includes 6 blocks of task and 6 blocks of rest. The duration of the task block and the rest block is 12 and 28 seconds, respectively

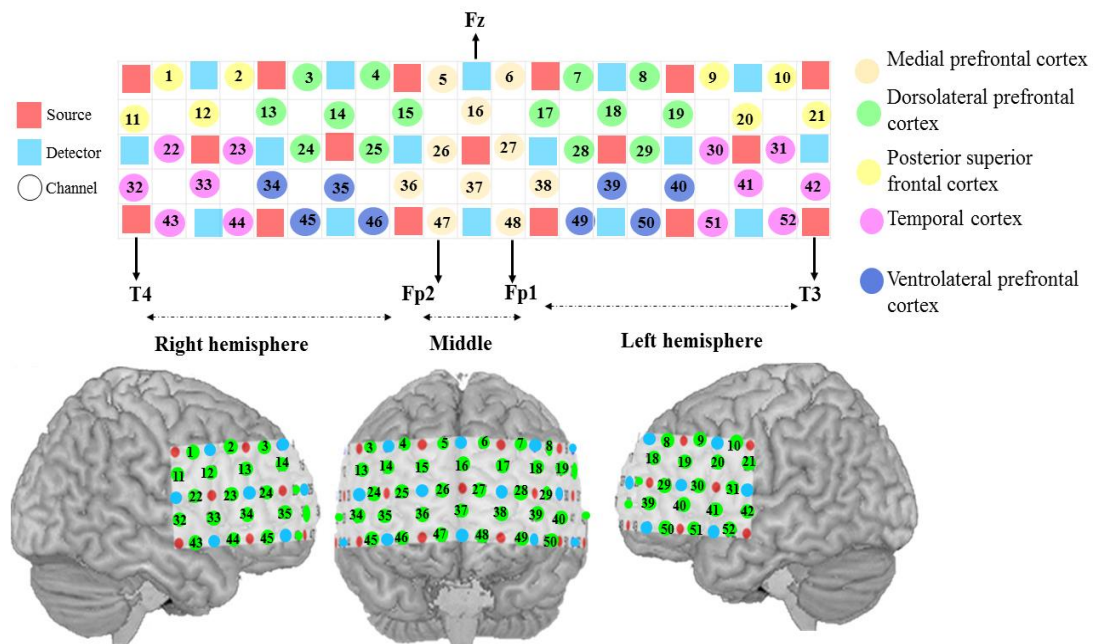


Figure 2. The distribution of the 52 channels and the placement of the light sources and detectors on the regions of the forehead and the temple, according to the international system of 10-20. Red, blue, and other colored points (orange, green, yellow, purple, dark blue) represent the position of sources, detectors, and channels along with their numbers, respectively

Table 1. The placement of channels in different regions of the forehead on the right and left hemispheres

Region	Channel Number
DLPFC Right	3,4,13,14,15,24,25
DLPFC Left	7,8,17,18,19,28,29
PSFC Right	1,2,11,12
PSFC Left	9,10,20,21
Temporal Right	22,23,32,33,43,44
Temporal Left	30,31,41,42,51,52
VLPFC Right	34,35,45,46
VLPFC Left	39,40,49,50
MPFC Right	5, 26,36,47
MPFC Left	6,27,38, 48

2.3. Signal Processing Algorithm

Figure 3 summarizes the signal processing algorithm, which uses DWT for filtering the fNIRS signals. This method is seen in many studies for signal processing [16, 18, 30, 31, 36, 37]. Therefore, DWT is used to reduce physiological interference effects, better analyzing brain performance, and assessing hemodynamic signals.

Signals obtained from fNIRS measure the alterations in brain tissue blood flow based on alterations in light absorption in tissues. These alterations represent brain activities. Since the measured light must pass through layers of the scalp, alterations in the blood flow of the superficial layers lead to interferences in fNIRS measurements. These interferences include physiological alterations such as changes in heart rate, breathing, Mayer wave, and very low oscillations in the frequency range of 0.8 to 1.2, 0.1 to 0.5, 0.1, and 0.04 Hz, respectively [12, 18, 38]. These physiological interferences may be taken for brain activity by mistake, reducing the accuracy of brain activity measurement. Among different filters investigated in the literature, DWT was successful in removing physiological interferences and improving SNR [16, 18, 30, 32, 39].

2.3.1. Discrete Wavelet Transform-Based Preprocessing

Wavelet Transforms are among the tools that have many applications in signal and image processing. Wavelet transform is the decomposition of a function based on the mother wavelet functions [40, 41]. DWT is an effective multilevel analysis tool in the time-frequency domain for signal analysis [32, 36, 39, 42, 43]. Wavelet coefficients are calculated by shifting and dilating the mother wavelet on signal $x(t)$. Then, by choosing appropriate coefficients in the desired frequency ranges, the given signal will be reconstructed in the time domain.

By repeatedly decomposing $x(t)$ and passing it through low-pass and high-pass filters, DWT creates a set of approximation and detail coefficients, each of which has a different frequency band [16, 18, 29]. DWT is obtained in M points using Equation 1 [32].

$$S[n] = \frac{1}{\sqrt{M}} \sum_k A_\phi [j_0, k] \Phi_{j_0, k}[n] + \frac{1}{\sqrt{M}} \sum_{j=j_0}^{\infty} \sum_k D_\psi [j, k] \Psi_{j, k}[n] \quad (1)$$

Where $\Phi_{j_0, k}[n]$ and $\Psi_{j, k}[n]$ represent scaling and the mother wavelet, respectively, and the latter is defined using Equation 2:

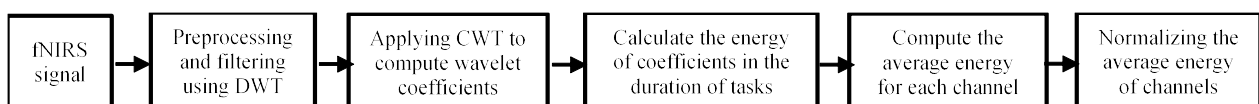
$$\Psi_{j, k}[n] = \frac{1}{\sqrt{j}} \psi \left(\frac{n-k}{j} \right) \quad (2)$$

Where j is the scaling parameter and k is the decomposition level. The inner product of these functions yields approximation coefficients (in low frequencies) and detail coefficients (in high frequencies) according to Equation 3 and Equation 4:

$$A_\phi [j_0, k] = \frac{1}{\sqrt{M}} \sum_n S[n] \Phi_{j_0, k}[n] \quad (3)$$

$$a_{j_0} = \frac{1}{\sqrt{M}} \sum_n A_\phi [j_0, k] \Phi_{j_0, k}[n] \quad (4)$$

$$D_\psi [j, k] = \frac{1}{\sqrt{M}} \sum_n S[n] \Psi_{j, k}[n]$$

**Figure 3.** Steps of the signal processing method

$$d_j = \frac{1}{\sqrt{M}} \sum_k D_\psi[j, k] \Psi_{j,k}[n]$$

Therefore, Equation 1 can be rewritten using a set of approximation and detail coefficients as Equation 5:

$$S[n] = a_{j_0} + \sum_j d_j \quad (5)$$

The appropriate choice of mother wavelet plays a pivotal role in the quality of the extraction and analysis of fNIRS signals from background noise [16, 44], depending on its similarity to the main signal, the shape of wavelet in the time domain, and its length [16, 18, 39, 40, 42, 43]. Considering what is mentioned, db5 mother wavelet is used for fNIRS signal decomposition in this study [16, 36]. The sampling rate is 10 Hz, and the frequency range for analyzing brain activation signals is 3 to 80 mHz [31]. Considering the Nyquist rate and sampling rate, HbO₂ and Hb signals are decomposed to 11 levels for brain activation analysis. In order to remove physiological interferences and considering their frequency bands, detail coefficients at the first six levels are considered zero, and for removing the DC, the 11th level approximation coefficient is also considered zero. The signals, then, are reconstructed in the time domain applying inverse wavelet transform. The filtered signal has a frequency content of 3 to 80 mHz.

2.3.2. Continuous Wavelet Transform

As previously stated, wavelet transform is a useful tool for signal analysis, and contrary to the Fourier Transform (FT), has windows with variable widths that can store time information of the signal [45]. According to the algorithm presented in Figure 3, wavelet coefficients are calculated using CWT, and the CWT of $x(t)$ is defined as the inner product in Equation 6.

$$W_x^\psi(s, \tau) = \langle x(t), \psi_{x,t}(t) \rangle = \frac{1}{\sqrt{|s|}} \int_{-\infty}^{\infty} x(t) \psi^* \left(\frac{t - \tau}{s} \right) dt \quad (6)$$

Where $\psi^*(t)$ represents the complex conjugate of mother wavelet $\psi(t)$, and s and τ represent scaling and translation parameters, respectively [36, 39, 46]. Presenting a 2-D representation of the signal in the time-scale domain, CWT represents $x(t)$ using the mother wavelet in different positions and scales. The wavelet transform coefficients of the signals are calculated using Equation 6.

After filtering the signal in the frequency range of 3 to 80 mHz, CWT is applied to the filtered signal, and

the CWT coefficients are calculated in 12-second time-steps (duration of doing the task) using this analysis. The obtained coefficients, therefore, include a set of task signal coefficients. In this study, the db5 mother wavelet is used for calculating the CWT coefficients, and considering these coefficients, the set of coefficients for each channel is created as follows (Equation 7):

$$W_j = [w_1, w_2, w_3, \dots, w_n], \quad (7)$$

$$n = 18 \text{ or } 24, j = 1, 2, \dots, 52$$

Where n and j represent the number of each task and channel, respectively. Then, the energies of every coefficient obtained in each task for HbO₂ and Hb signals are calculated according to Equation 9.

2.3.3. Calculation of Wavelet Energy

In general, the energy of a time signal, $x(t)$, is calculated as Equation 8:

$$E = \int_{-\infty}^{\infty} |x(t)|^2 dt = \|x(t)\|^2 \quad (8)$$

Also, the energy density function of the 2-D wavelet transform is used according to Equation 9 to calculate the energy of wavelet transform coefficients in scale s and location τ [47].

$$E(s, \tau) = |w(s, \tau)|^2 \quad (9)$$

Hence, for each channel, there are 18 or 24 tasks, and the energy of each task for each channel is calculated. Next, the average energy of all tasks for each channel was calculated, which yielded 52 indices, each representing the average energy of a channel. Finally, they are normalized using Equation 10.

$$\langle E \rangle_{N,j} = \frac{\langle E \rangle_j}{\max\{\langle E \rangle_1, \langle E \rangle_2, \dots, \langle E \rangle_{52}\}} \quad (10)$$

Where $\langle E \rangle_{N,j}$ is the normalized average energy of each channel, $\langle E \rangle_j$ is the average energy of each channel, and $\max\{\langle E \rangle_1, \langle E \rangle_2, \dots, \langle E \rangle_{52}\}$ is the maximum channel energy.

After normalizing the average energy of channels, the t-test is used for identifying significant differences between the energy of symmetric channel pairs in all subjects for each HbO₂ and Hb signal ($P < 0.05$).

3. Results

fNIRS signals contain information on brain activation in different regions of the brain under mental arithmetic tasks. In this study, we applied CWT to fNIRS signals to analyze these activities in different regions of the brain. After removing physiological interferences from fNIRS signals of the left and right hemispheres, filtered signals were prepared for the following processes. The desirable signal contains a set of task and rest signals. Figure 4 shows an example of HbO₂ and Hb signal after removing physiological interferences. Blue and white rectangles represent task and rest blocks, respectively. It is shown in Figure 4 that the desirable signal contains 18 task and rest blocks.

First, wavelet coefficients of HbO₂ and Hb signals in eight subjects were calculated in the time-frequency domain by applying CWT to task signals. Then, the energy of each wavelet coefficient during each task, along with the average energy of coefficients of all tasks in each channel for each subject, was calculated, resulting in a 52-element vector for each subject, with each element corresponding to a channel. Overall, an 8×52 matrix was obtained for 8 subjects, its rows representing subjects and columns channels. Finally, the energy of all channels in a subject was normalized to a number between zero and one. The average energy matrix of HbO₂ and Hb signals in the time-frequency domain by applying CWT are shown in Figure 5a and Figure 5b that red and blue represent the maximum and minimum value of normalized energy, respectively.

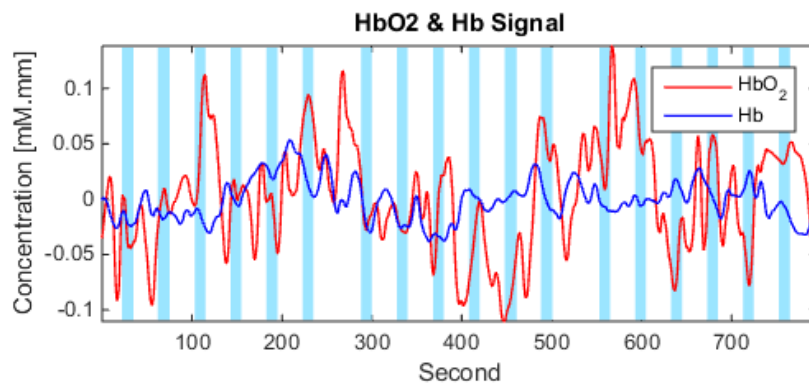


Figure 4. HbO₂ and Hb signal after filtering. Blue and white colors indicate task and rest blocks, respectively. The signal includes three runs or 18 task blocks

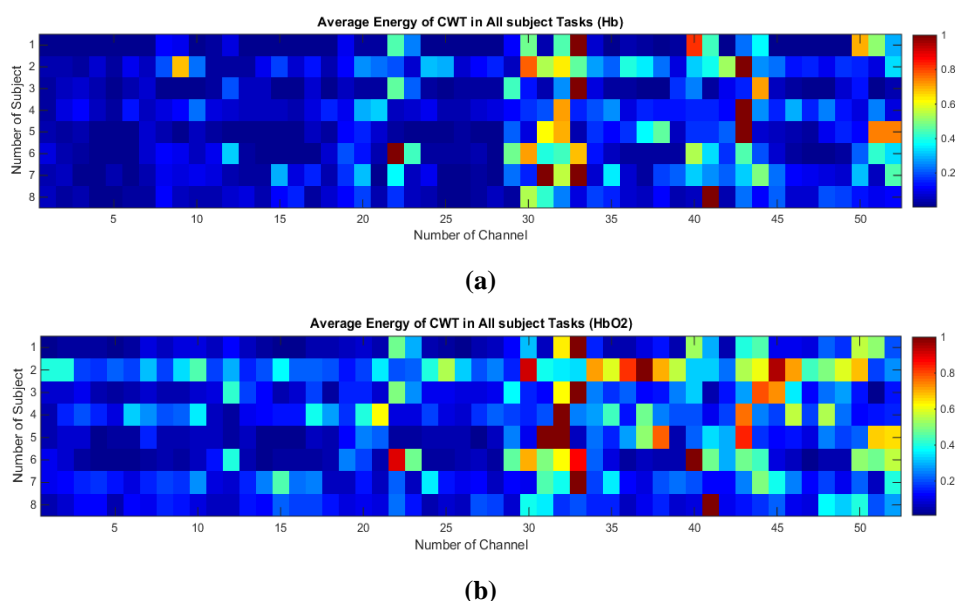


Figure 5. The average energy of fNIRS signals in the time-frequency domain by applying CWT: (a) the average energy of oxyhemoglobin signal among all subjects in each channel. (b) The average energy of deoxyhemoglobin signal of all subjects in each channel. Rows and columns represent subjects and channels, respectively

The t-test is applied to HbO₂ signals between every symmetric channel pairs on the two hemispheres for all subjects, except for channels 16 and 37 which were omitted because of their positioning on the corpus callosum. As seen in Table 2, the following symmetric channel pairs showed significant differences: the channel pair corresponding to 7 on the left hemisphere and 4 on the right hemisphere (P=0.04) in the DLPFC region; the channel pair corresponding to 48 on the left hemisphere and 47 on the right hemisphere (P=0.009) in the MPFC region; the channel pair corresponding to 42 and 32 (P=0.003) in the temporal region.

Figure 5b shows the average energy matrix for Hb signal. Also, the t-test was applied to Hb signals of symmetric channel pairs on the two hemispheres of all subjects. As seen in Table 3, the following symmetric channel pairs also showed significant differences compared to other channels in their regions: the channel pair corresponding to 50 on the left hemisphere and 45 on the right hemisphere (P=0.031) in the VLPFC; the channel pair corresponding to 6 on the left hemisphere and 5 on the right hemisphere (P=0.027) in the MPFC region; the channel pair corresponding to 42 and 32 (P=0.007) on the temporal region. Therefore, the average energy of signals was greater on the left hemisphere in the DLPFC and MPFC regions in HbO₂ signal and in the VLPFC and MPFC regions in Hb signal, compared to the temporal region on the right hemisphere. The average and variance of HbO₂ and Hb signals of each channel are

presented in Tables 2 and 3. The results indicate that the temporal, DLPFC, VLPFC, and MPFC regions in the frontal cortex play a crucial role in cognitive processes during arithmetic tasks.

4. Discussion

The goal of this research is to study the activation of different regions in the PFC under the mental arithmetic tasks. fNIRS signal coefficients were calculated for each subject and each task using CWT analysis which can detect signal alterations in the time-frequency band. After calculating the energy of CWT coefficients in the time period of tasks and frequency range of 3 to 80 mHz, the average energy of all tasks in each channel of each subject was calculated. Next, the energy of symmetric channels in the two hemispheres was compared using the t-test, which yields the activation of different regions in the PFC. The results showed a significant increase of the PFC activation in both signals of a channel pair placed in the temporal and MPFC regions.

HbO₂ and Hb signals in the subjects were measured simultaneously for assessing the PFC activation in different channels. Studies have indicated alterations in the concentration of Hb and HbO₂ signals in the PFC caused by brain activation and physiological performance under cognitive tasks [7, 48, 49]. So, subjects were asked to subtract one-digit numbers from two-digit numbers

Table 2. The average and variance values of HbO₂ signal in the right and left hemispheres

HbO ₂ Signal					
Region	P-value	Left Channel	Right Channel	Left Channel (Mean ± Var)	Right Channel (Mean ± Var)
DLPFC	0.040	7	4	0.152 ± 0.009	0.094 ± 0.004
Temporal	0.003	42	32	0.180 ± 0.008	0.598 ± 0.085
MPFC	0.009	48	47	0.295 ± 0.027	0.152 ± 0.015

Table 3. The average and variance of Hb signal in the right and left hemispheres

Hb signal					
Region	P-value	Left Channel	Right Channel	Left Channel (Mean ± Var)	Right Channel (Mean ± Var)
MPFC	0.027	6	5	0.114 ± 0.015	0.055 ± 0.008
Temporal	0.007	42	32	0.154 ± 0.027	0.523 ± 0.047
VLPFC	0.031	50	45	0.312 ± 0.058	0.068 ± 0.005

as a mental task. The role of the PFC, in solving mental arithmetic tasks and its relationship with different active brain cortices under this task, is among crucial subjects in cognitive sciences [50]. The PFC is an important part of the nervous system, playing a major role in solving arithmetic problems and different cognitive functions such as storing information, working memory, attention, and other functions [50-53]. Therefore, this task is widely used as a cognitive process for studying the arithmetic ability of subjects, and it requires complex neural networks for accurate calculations [54, 55]. This task also activates neural networks in different cortical regions both locally and spatially [55].

After filtering the signals and applying the CWT, the energies of HbO₂ and Hb signals were calculated, followed by the extraction of 18 or 24 sets of coefficients for each channel in every subject. These sets of coefficients include the wavelet coefficients of task signals in the time period of 12 seconds and frequency range of 3 to 80 mHz. Following the calculation of the energy of these sets of coefficients in every channel, their average values were calculated. Finally, for demonstrating statistically significant differences between symmetric channel pairs in both hemispheres, the t-test was applied to both HbO₂ and Hb signals. This study showed interesting results regarding the effects of the cognitive task on brain activation. The most significant activated regions in both HbO₂ and Hb signals include the medial region in the left hemisphere and the temporal region in the right hemisphere. The results indicate an activation pattern between left and right regions in both HbO₂ and Hb signals. As presented in Tables 2 and 3, the left hemisphere is significantly more active than the right hemisphere while doing arithmetic operations. The channel pair corresponding to channels 4 and 7 on the right and left hemispheres in the DLPFC, respectively, showed significant activation in HbO₂ signal. Also, the channel pair corresponding to channels 45 and 50 on the right and left hemispheres in the VLPFC, respectively, showed significant activation in Hb signal. Previous studies done by fMRI demonstrated enhanced brain activation in different cortical regions [56-59] such as the PFC, including the DLPFC and VLPFC [60-62], under the mental arithmetic tasks, along with increased activation in the anterior cingulate region [61]. These observations are in line with our results. Since different strategies can be adopted for doing the subtractions, a high level of activation can be observed in this cognitive task. This study showed that the left hemisphere is directly related to arithmetic operations.

In accordance with study [63], the left hemisphere of the PFC showed more activation than the right hemisphere, which may indicate that accurate and detailed calculations are processed in the left hemisphere since the left hemisphere is responsible for mathematics and logical and analytical data processing while the right hemisphere does general and comprehensive processing [64]. Furthermore, some studies have shown that different factors such as the difficulty of the task, the recognition of mathematical operations, and the solving method can lead to significantly different activation patterns in different brain regions such as the PFC [65, 66].

As mentioned earlier, the increased concentration of oxygen under the cognitive task indicates an increase in the activation level in all parts of the PFC. Our results illustrate that the DLPFC is constantly activated with mental calculations, which is supported by the findings of Vassena *et al.* [35]. Also, assessing time patterns of the hemodynamic response of HbO₂ and Hb signals in different brain regions under mental arithmetic task using fNIRS, in study [33], has shown a rise in HbO₂ signal in the DLPFC along with a drop in the medial area of the Anterior Prefrontal Cortex (APFC). Considering the DLPFC activation features, this region is a member of the nervous system responsible for synchronizing mental processes [26, 67], and performing subtractions and storing numbers, cognitive control, and selection processes trigger its activation. The DLPFC plays a pivotal role in preparation for a cognitive task such as a mental arithmetic task and memorizing abstract information on rules governing the tasks [35], while also playing a role in cognitive functions such as working memory, strategic organization during encoding, and response selection [57, 68]. Furthermore, the VLPFC's role is also in cognitive functions of the working memory such as encoding and restoring while the DLPFC has a more distinct role such as supervision or modification in the content of the working memory [60].

In addition to the DLPFC activation, brain activation was observed in other regions including the temporal region where (32, 42) channel pair is located and the medial region where (47, 48) channel pair is located. The temporal lobe has a vital role in memory storage and processing data [69]. Considering the capability of fMRI in detecting the activation of the temporal regions in some subjects, findings [57-59] are in line with our findings. Furthermore, Vassena *et al.* [35] suggest that

the MPFC activation, which occurs due to reward expectation, is controlled by the DLPFC.

In the study [33], the temporal-spatial patterns of HbO₂ and Hb responses in a specific period of two seconds (10 to 12 seconds) were investigated during a simple mental arithmetic task in prefrontal brain regions. In the preprocessing, they used a bandpass Butterworth filter in the frequency range from 0.01 Hz to 0.09 Hz to reduce artifacts and remove baseline drifts. Then, averaging methods were used to analyze the signals in the focal points of the brain in the prefrontal cortex. Then, the mean task-related concentration changes of HbO₂ and Hb were calculated for focal frontal HbO₂ and Hb responses. In the present study, the aim is to investigate and compare the time-frequency behavior of the hemodynamic response of symmetric spatial activity on two cerebral hemispheres by using CWT. Initially, DWT was used to reduce physiological noise in the frequency range of 0.003 to 0.08 Hz. Then, CWT was applied to analyze concentration changes of Hb and HbO₂ signals in symmetrical channels on the two hemispheres. Finally, the mean of the wavelet coefficients as energy at the 12-second interval of the task was calculated. In the mentioned studies, brain activation levels were analyzed using HbO₂ signals because Hb signal is weaker than HbO₂ and has a smaller signal to noise ratio. In [33], due to the small amplitude of Hb signal, the analysis of Hb signal did not show significant results. However, the current study analyzed both signals, demonstrating that Hb signals also provide useful information on brain activation. As a result, significant results were observed in Hb data using CWT method. Also, HbO₂ and Hb show similar results in the two regions (See Tables 2 and 3).

Generally, frontal cortex activation can be attributed to several cognitive functions such as attention, encoding and restoring memory, decision-making, and storing numbers in the working memory, each of which is related to a specific region in the brain, such as the temporal region or the DLPFC [50-53]. Despite presenting significant results associated with alterations in HbO₂ and Hb signals under mental arithmetic tasks, this study also has some limitations. For instance, slow neuronal activity leads to changes in hemodynamic patterns. Also, the PFC has a complex structure, so it is possible for some channels not to function distinctively and represent other functions as well [33]. Finally, another limitation is the number of subjects. Due to personal differences, different brain

function activation patterns occur in different subjects, which means that a larger number of subjects is needed for more precise analyses. However, despite such limitations, activated regions in this study were observable by both fMRI and fNIRS. Therefore, this technique can be known as an effective method for analyzing active brain regions, especially in the frontal cortex, under mental arithmetic tasks, considering the features of fNIRS. Furthermore, the acceptable temporal and spatial precision of this imaging technique enables us to better detect and understand active regions in cognitive functions.

5. Conclusion

This paper studied the frontal cortex activation of healthy subjects under the mental arithmetic tasks using fNIRS. We analyzed the energy of the signal in different regions of the frontal cortex in both HbO₂ and Hb signals, and the location of channels with significant differences, in both HbO₂ and Hb signals, were determined. The results show that cognitive processes are directly associated with and play an important role in the activation of the frontal cortex. Also, brain activation was more significant in the frontal cortex, especially in the left hemisphere, where extensive activation was observed in attention, performance, and working memory functions. This region was also activated with working memory and logical thinking. Therefore, it can be concluded from this study that fNIRS was successfully able to scrutinize the activation of different brain regions.

References

- 1- M. M. Faskhodi, Z. Einalou, and M. Dadgostar, "Diagnosis of Alzheimer's disease using resting-state fMRI and graph theory," *Technology and Health Care*, vol. 26, no. 6, pp. 921-931, 2018.
- 2- S. Cutini, S. B. Moro, and S. Bisconti, "Functional near infrared optical imaging in cognitive neuroscience: an introductory review," *Journal of Near Infrared Spectroscopy*, vol. 20, no. 1, pp. 75-92, 2012.
- 3- Y. Joannette, A. I. Ansaldo, M. A. de Mattos Pimenta Parente, R. P. Fonseca, C. H. Kristensen, and L. C. Scherer, "Neuroimaging investigation of executive functions: Evidence from fNIRS," *Psico*, 2008.
- 4- S. Barahimi, Z. Einalou, and M. Dadgostar, "Studies on schizophrenia and depressive diseases based on functional near-infrared spectroscopy," *Biomedical Engineering*:

- Applications, Basis and Communications*, vol. 30, no. 04, p. 1830002, 2018.
- 5- F. Irani, S. M. Platek, S. Bunce, A. C. Ruocco, and D. Chute, "Functional near infrared spectroscopy (fNIRS): an emerging neuroimaging technology with important applications for the study of brain disorders," *The Clinical Neuropsychologist*, vol. 21, no. 1, pp. 9-37, 2007.
 - 6- A. Mirelman *et al.*, "Increased frontal brain activation during walking while dual tasking: an fNIRS study in healthy young adults," *Journal of neuroengineering and rehabilitation*, vol. 11, no. 1, p. 85, 2014.
 - 7- M. Tanida, K. Sakatani, R. Takano, and K. Tagai, "Relation between asymmetry of prefrontal cortex activities and the autonomic nervous system during a mental arithmetic task: near infrared spectroscopy study," *Neuroscience letters*, vol. 369, no. 1, pp. 69-74, 2004.
 - 8- A. R. Sonkaya, "The Use of Functional Near Infrared Spectroscopy Technique in Neurology," *NeuroQuantology*, vol. 16, no. 7, 2018.
 - 9- H. Y. Kim, K. Seo, H. J. Jeon, U. Lee, and H. Lee, "Application of functional near-infrared spectroscopy to the study of brain function in humans and animal models," *Molecules and cells*, vol. 40, no. 8, p. 523, 2017.
 - 10- M. Soltanlou, M. A. Sitnikova, H.-C. Nuerk, and T. Dresler, "Applications of functional near-infrared spectroscopy (fNIRS) in studying cognitive development: the case of mathematics and language," *Frontiers in psychology*, vol. 9, p. 277, 2018.
 - 11- J. B. Balardin *et al.*, "Imaging brain function with functional near-infrared spectroscopy in unconstrained environments," *Frontiers in human neuroscience*, vol. 11, p. 258, 2017.
 - 12- F. Herold, P. Wiegel, F. Scholkmann, and N. Müller, "Applications of Functional Near-Infrared Spectroscopy (fNIRS) Neuroimaging in Exercise–Cognition Science: A Systematic, Methodology-Focused Review," *Journal of clinical medicine*, vol. 7, no. 12, p. 466, 2018.
 - 13- D. A. Boas, C. E. Elwell, M. Ferrari, and G. Taga, "Twenty years of functional near-infrared spectroscopy: introduction for the special issue," ed: Elsevier, 2014.
 - 14- F. Scholkmann *et al.*, "A review on continuous wave functional near-infrared spectroscopy and imaging instrumentation and methodology," *Neuroimage*, vol. 85, pp. 6-27, 2014.
 - 15- M. Wolf, M. Ferrari, and V. Quaresima, "Progress of near-infrared spectroscopy and topography for brain and muscle clinical applications," *Journal of biomedical optics*, vol. 12, no. 6, p. 062104, 2007.
 - 16- Z. Einalou, K. Maghooli, S. K. Setarehdan, and A. Akin, "Graph theoretical approach to functional connectivity in prefrontal cortex via fNIRS," *Neurophotronics*, vol. 4, no. 4, p. 041407, 2017.
 - 17- N. Masataka, L. Perlovsky, and K. Hiraki, "Near-infrared spectroscopy (NIRS) in functional research of prefrontal cortex," *Frontiers in human neuroscience*, vol. 9, p. 274, 2015.
 - 18- M. Dadgostar, S. K. Setarehdan, S. Shahzadi, and A. Akin, "Functional connectivity of the PFC via partial correlation," *Optik*, vol. 127, no. 11, pp. 4748-4754, 2016.
 - 19- M. Dadgostar, S. K. Setarehdan, S. Shahzadi, and A. Akin, "Classification of schizophrenia using SVM via fNIRS," *Biomedical Engineering: Applications, Basis and Communications*, vol. 30, no. 02, p. 1850008, 2018.
 - 20- N. Okamoto, Y. Kuroda, B. Chance, S. Nioka, H. Eda, and T. Maesako, "Measurement of brain activation difference during different mathematical tasks by near infrared spectroscopy," in *Optical Tomography and Spectroscopy of Tissue VIII*, 2009, vol. 7174, p. 71741M: International Society for Optics and Photonics.
 - 21- H. Meiri *et al.*, "Frontal lobe role in simple arithmetic calculations: An fNIR study," *Neuroscience letters*, vol. 510, no. 1, pp. 43-47, 2012.
 - 22- C. Herff, D. Heger, F. Putze, J. Hennrich, O. Fortmann, and T. Schultz, "Classification of mental tasks in the prefrontal cortex using fNIRS," in *2013 35th Annual International Conference of the IEEE Engineering in Medicine and Biology Society (EMBC)*, 2013, pp. 2160-2163: IEEE.
 - 23- S. D. Power, T. H. Falk, and T. Chau, "Classification of prefrontal activity due to mental arithmetic and music imagery using hidden Markov models and frequency domain near-infrared spectroscopy," *Journal of neural engineering*, vol. 7, no. 2, p. 026002, 2010.
 - 24- N. Naseer and K.-S. Hong, "Classification of functional near-infrared spectroscopy signals corresponding to the right-and left-wrist motor imagery for development of a brain–computer interface," *Neuroscience letters*, vol. 553, pp. 84-89, 2013.
 - 25- H. Ohsugi, S. Ohgi, K. Shigemori, and E. B. Schneider, "Differences in dual-task performance and prefrontal cortex activation between younger and older adults," *BMC neuroscience*, vol. 14, no. 1, p. 10, 2013.
 - 26- M. Verner, M. J. Herrmann, S. J. Troche, C. M. Roebers, and T. H. Rammsayer, "Cortical oxygen consumption in mental arithmetic as a function of task difficulty: a near-infrared spectroscopy approach," *Frontiers in human neuroscience*, vol. 7, p. 217, 2013.
 - 27- P. Pinti, D. Cardone, and A. Merla, "Simultaneous fNIRS and thermal infrared imaging during cognitive task reveal autonomic correlates of prefrontal cortex activity," *Scientific reports*, vol. 5, no. 1, pp. 1-14, 2015.

- 28- L. Duan, Z. Zhao, Y. Lin, X. Wu, Y. Luo, and P. Xu, "Wavelet-based method for removing global physiological noise in functional near-infrared spectroscopy," *Biomedical optics express*, vol. 9, no. 8, pp. 3805-3820, 2018.
- 29- S. Shirzadi, Z. Einalou, and M. Dadgostar, "Investigation of functional connectivity during working memory task and hemispheric lateralization in left-and right-handers measured by fNIRS," *Optik*, vol. 221, p. 165347, 2020.
- 30- B. Molavi and G. A. Dumont, "Wavelet-based motion artifact removal for functional near-infrared spectroscopy," *Physiological measurement*, vol. 33, no. 2, p. 259, 2012.
- 31- Z. Einalou, K. Maghooli, S.-K. Setarehdan, and A. Akin, "Functional near infrared spectroscopy to investigation of functional connectivity in schizophrenia using partial correlation," *Univers. J. Biomed. Eng.*, vol. 2, no. 1, pp. 5-8, 2014.
- 32- T. Trakoolwilaiwan, B. Behboodi, J. Lee, K. Kim, and J.-W. Choi, "Convolutional neural network for high-accuracy functional near-infrared spectroscopy in a brain-computer interface: three-class classification of rest, right-, and left-hand motor execution," *Neurophotonics*, vol. 5, no. 1, p. 011008, 2017.
- 33- G. Pfurtscheller, G. Bauernfeind, S. C. Wriessnegger, and C. Neuper, "Focal frontal (de) oxyhemoglobin responses during simple arithmetic," *International Journal of Psychophysiology*, vol. 76, no. 3, pp. 186-192, 2010.
- 34- G. Bauernfeind, R. Scherer, G. Pfurtscheller, and C. Neuper, "Single-trial classification of antagonistic oxyhemoglobin responses during mental arithmetic," *Medical & biological engineering & computing*, vol. 49, no. 9, pp. 979-984, 2011.
- 35- E. Vassena, R. Gerrits, J. Demanet, T. Verguts, and R. Siugzdaite, "Anticipation of a mentally effortful task recruits Dorsolateral Prefrontal Cortex: An fNIRS validation study," *Neuropsychologia*, vol. 123, pp. 106-115, 2019.
- 36- M. Dadgostar, S. Setarehdan, and A. Akin, "Detection of motion artifacts in fNIRS via the continuous wavelet transform," in *2013 20th Iranian Conference on Biomedical Engineering (ICBME)*, 2013, pp. 243-246: IEEE.
- 37- Z. Einalou, K. Maghooli, S. K. Setarehdan, and A. Akin, "Effective channels in classification and functional connectivity pattern of prefrontal cortex by functional near infrared spectroscopy signals," *Optik*, vol. 127, no. 6, pp. 3271-3275, 2016.
- 38- H. Obrig et al., "Spontaneous low frequency oscillations of cerebral hemodynamics and metabolism in human adults," *Neuroimage*, vol. 12, no. 6, pp. 623-639, 2000.
- 39- H. Tsunashima, K. Yanagisawa, and M. Iwadate, "Measurement of brain function using near-infrared spectroscopy (NIRS)," in *Neuroimaging-Methods: IntechOpen*, 2012.
- 40- S. Hamideh, E. Zahra, D. Mehrdad, and M. Keivan, "Classification of SSVEP-based BCIs using Genetic Algorithm," *Journal of Big Data*, vol. 8, no. 1, 2021.
- 41- S. G. Oskoei, M. Dadgostar, G. R. Rad, and E. Fatemizadeh, "Adaptive watermarking scheme based on ICA and RDWT," 2009.
- 42- L. Mohammadi, Z. Einalou, H. Hosseinzadeh, and M. Dadgostar, "Cursor movement detection in brain-computer-interface systems using the K-means clustering method and LSVM," *Journal of Big Data*, vol. 8, no. 1, pp. 1-15, 2021.
- 43- B. Abibullaev, J. An, and J.-I. Moon, "Neural network classification of brain hemodynamic responses from four mental tasks," *International Journal of Optomechatronics*, vol. 5, no. 4, pp. 340-359, 2011.
- 44- S. Roldan-Vasco, E. Perez-Giraldo, and A. Orozco-Duque, "Continuous Wavelet Transform for Muscle Activity Detection in Surface EMG Signals During Swallowing," in *International Workshop on Experimental and Efficient Algorithms*, 2018, pp. 245-255: Springer.
- 45- C. Torrence and G. P. Compo, "A practical guide to wavelet analysis," *Bulletin of the American Meteorological society*, vol. 79, no. 1, pp. 61-78, 1998.
- 46- B. Abibullaev and J. An, "Classification of frontal cortex haemodynamic responses during cognitive tasks using wavelet transforms and machine learning algorithms," *Medical engineering & physics*, vol. 34, no. 10, pp. 1394-1410, 2012.
- 47- P. S. Addison, *The illustrated wavelet transform handbook: introductory theory and applications in science, engineering, medicine and finance*. CRC press, 2017.
- 48- Y. Hoshi et al., "Non-synchronous behavior of neuronal activity, oxidative metabolism and blood supply during mental tasks in man," *Neuroscience letters*, vol. 172, no. 1-2, pp. 129-133, 1994.
- 49- Y. Hoshi and M. Tamura, "Detection of dynamic changes in cerebral oxygenation coupled to neuronal function during mental work in man," *Neuroscience letters*, vol. 150, no. 1, pp. 5-8, 1993.
- 50- S. Hashim, N. M. Safri, M. A. Othman, and N. A. Zakaria, "Brain functional connectivity and power spectrum analyses during mental arithmetic," *Jurnal Teknologi*, vol. 74, no. 6, pp. 41-47, 2015.
- 51- V. Menon, "Developmental cognitive neuroscience of arithmetic: implications for learning and education," *Zdm*, vol. 42, no. 6, pp. 515-525, 2010.

- 52- T. Fehr, C. Code, and M. Herrmann, "Common brain regions underlying different arithmetic operations as revealed by conjunct fMRI–BOLD activation," *Brain research*, vol. 1172, pp. 93-102, 2007.
- 53- T. Dresler *et al.*, "Arithmetic tasks in different formats and their influence on behavior and brain oxygenation as assessed with near-infrared spectroscopy (NIRS): a study involving primary and secondary school children," *Journal of neural transmission*, vol. 116, no. 12, p. 1689, 2009.
- 54- J. Yu, Y. Pan, K. K. Ang, C. Guan, and D. J. Leamy, "Prefrontal cortical activation during arithmetic processing differentiated by cultures: A preliminary fNIRS study," in *2012 Annual International Conference of the IEEE Engineering in Medicine and Biology Society*, 2012, pp. 4716-4719: IEEE.
- 55- Y. Murata *et al.*, "Comparison of Cortical Activation during Subtraction in Mental Calculation and with a Calculator," *Biochemistry and Analytical Biochemistry*, vol. 4, no. 3, p. 1, 2015.
- 56- V. Menon, S. Rivera, C. White, G. Glover, and A. Reiss, "Dissociating prefrontal and parietal cortex activation during arithmetic processing," *Neuroimage*, vol. 12, no. 4, pp. 357-365, 2000.
- 57- L. Rueckert *et al.*, "Visualizing cortical activation during mental calculation with functional MRI," *Neuroimage*, vol. 3, no. 2, pp. 97-103, 1996.
- 58- O. Gruber, P. Indefrey, H. Steinmetz, and A. Kleinschmidt, "Dissociating neural correlates of cognitive components in mental calculation," *Cerebral cortex*, vol. 11, no. 4, pp. 350-359, 2001.
- 59- R. Kawashima *et al.*, "A functional MRI study of simple arithmetic—a comparison between children and adults," *Cognitive Brain Research*, vol. 18, no. 3, pp. 227-233, 2004.
- 60- D. Bor and A. M. Owen, "A common prefrontal–parietal network for mnemonic and mathematical recoding strategies within working memory," *Cerebral cortex*, vol. 17, no. 4, pp. 778-786, 2006.
- 61- S. M. Rivera, A. Reiss, M. A. Eckert, and V. Menon, "Developmental changes in mental arithmetic: evidence for increased functional specialization in the left inferior parietal cortex," *Cerebral cortex*, vol. 15, no. 11, pp. 1779-1790, 2005.
- 62- T. Rickard, S. Romero, G. Basso, C. Wharton, S. Flitman, and J. Grafman, "The calculating brain: an fMRI study," *Neuropsychologia*, vol. 38, no. 3, pp. 325-335, 2000.
- 63- P. Burbaud, O. Camus, D. Guehl, B. Bioulac, J.-M. Caillé, and M. Allard, "A functional magnetic resonance imaging study of mental subtraction in human subjects," *Neuroscience letters*, vol. 273, no. 3, pp. 195-199, 1999.
- 64- A. N. Kitchens, "Left brain/right brain theory: Implications for developmental math instruction," *Review of Research in Developmental Education*, vol. 8, no. 3, p. n3, 1991.
- 65- D. Ansari, R. H. Grabner, K. Koschutnig, G. Reishofer, and F. Ebner, "Individual differences in mathematical competence modulate brain responses to arithmetic errors: An fMRI study," *Learning and Individual Differences*, vol. 21, no. 6, pp. 636-643, 2011.
- 66- V. Menon, K. Mackenzie, S. M. Rivera, and A. L. Reiss, "Prefrontal cortex involvement in processing incorrect arithmetic equations: Evidence from event-related fMRI," *Human brain mapping*, vol. 16, no. 2, pp. 119-130, 2002.
- 67- M. J. Vansteensel *et al.*, "Brain–computer interfacing based on cognitive control," *Annals of neurology*, vol. 67, no. 6, pp. 809-816, 2010.
- 68- J. Taillan, E. Ardiale, J.-L. Anton, B. Nazarian, O. Félician, and P. Lemaire, "Processes in arithmetic strategy selection: a fMRI study," *Frontiers in Psychology*, vol. 6, p. 61, 2015.
- 69- P. A. Abhang, B. W. Gawali, and S. C. Mehrotra, *Introduction to EEG-and speech-based emotion recognition*. Academic Press, 2016.